1-1-2014

Optical isolation via PT-symmetric nonlinear Fano resonances

F. Nazari

N. Bender

H. Ramezani

M. K. Moravvej-Farshi

D. N. Christodoulides
University of Central Florida

See next page for additional authors

Optical isolation via $\mathscr{P}\mathscr{T}$-symmetric nonlinear Fano resonances

F. Nazari,[1,2] N. Bender,[1] H. Ramezani,[1] M. K.Moravvej-Farshi,[2] D. N. Christodoulides,[3] and T. Kottos[1,4,*]

[1]*Department of Physics, Wesleyan University, Middletown, CT-06459, USA*

[2]*Faculty of Electrical & Computer Engineering, Tarbiat Modares University, Tehran 1411713116, Iran*

[3]*College of Optics & Photonics-CREOL, UCF, Orlando, Florida 32816, USA*

[4]*Max Planck Institute for Dynamics and Self-organization, 37077 Goettingen, Germany*

[*]*tkottos@wesleyan.edu*

Abstract: We show that Fano resonances created by two $\mathscr{P}\mathscr{T}$-symmetric nonlinear micro-resonators coupled to a waveguide, have line-shape and resonance position that depends on the direction of the incident light. We utilize these features in order to induce asymmetric transport, up to 47 dBs, in the optical C-window. Our theoretical proposal requires low input power and does not compromise the power or frequency characteristics of the output signal.

OCIS codes: (230.3240) Isolators; (000.6800) Theoretical physics; (130.0130) Integrated optics.

References and links

1. Z. Yu, S. Fan, "Complete optical isolation created by indirect interband photonic transitions," Nat. Photonics **3**, 91-94 (2009).
2. M.S. Kang, A. Butsch, and P.S.J. Russell," Reconfigurable light-driven opto-acoustic isolators in photonic crystal fibre," Nat. Photonics **5**, 549-553 (2011).
3. K. Gallo, G. Assanto,"All-optical diode based on second-harmonic generation in an asymmetric waveguide," JOSA B **16**, 267-269 (1999).
4. M. Scalora, J.P. Dowling, C.M. Bowden, and M.J. Bloemer, "The photonic band edge optical diode," J. Appl. Phys. **76**, 2023-2026 (1994).
5. S. Lepri, G. Casati, "Asymmetric wave propagation in nonlinear systems," Phys. Rev. Lett. **106**, 164101 (2011).
6. Y. Xu, A. E. Miroshnichenko, "Reconfigurable nonreciprocity with nonlinear Fano diode," eprint arXiv:1311.2533 (2013).
7. L. Fan, J. Wang, L.T. Varghese, H. Shen, B. Niu, Y. Xuan, A. M. Weiner, and M. Qi, "An all-silicon passive optical diode," Science **335**, 447-450 (2012).
8. B. Peng, S. K. Ozdemir, F. Lei, F. Monifi, M. Gianfreda, G. L. Long, S. Fan, F. Nori, C. M. Bender, and L. Yang, "Nonreciprocal light transmission in parity-time-symmetric whispering-gallery microcavities," arXiv:1308.4564 (2013).
9. K. J. Vahala, "Optical microcavities," Nature (London) **424**, 839-846 (2003).
10. N. Bender, S. Factor, J.D. Bodyfelt, H. Ramezani, D. N. Christodoulides, F. Ellis, and T. Kottos, "Observation of asymmetric transport in structures with active nonlinearities," Phys. Rev. Lett. **110**, 234101 (2013).
11. A. E. Miroshnichenko, S. Flach, and Y.S. Kivshar, "Fano resonances in nanoscale structures," Rev. Mod. Phys. **82**, 2257-2298 (2010).
12. K. Srinivasan, M. Borselli, O. Painter, A. Stintz, and S. Krishna, "Cavity Q, mode volume, and lasing threshold in small diameter AlGaAs microdisks with embedded quantum dots," Opt. Express **14**, 1094-1105 (2006).
13. C. M. Bender, "Making sense of non-hermitian hamiltonians," Rep. Prog. Phys. **70**, 947-1018 (2007).

#207316 - $15.00 USD Received 27 Feb 2014; revised 28 Mar 2014; accepted 30 Mar 2014; published 14 Apr 2014

14. The $\mathscr{P}\mathscr{T}$-symmetric phase transition can be also achieved by manipulating the coupling strength between the gain an loss elements while keeping the balanced gain and loss parameter constant. Specifically it can be shown that decreasing the coupling strength is equivalent to increasing the gain and loss parameter.
15. K. G. Makris, R. El-Ganainy, and D.N. Christodoulides, "Beam dynamics in PT symmetric optical lattices," Phys. Rev. Lett. **100**, 103904 (2008).
16. C. E. Rüter, K. G. Makris, R. El-Ganainy, D. N. Christodoulides, M. Segev, and D. Kip, "Observation of parity-time symmetry in optics," Nat. Phys. **6**, 192-195 (2010).
17. A. Regensburger, C. Bersch, M.A. Miri, G. Onishchukov, D. N. Christodoulides, and U. Peschel, "Parity - time synthetic photonic lattices," Nature **488**, 167-171 (2012).
18. S. Longhi, "PT-symmetric laser absorber," Phys. Rev. A **82**, 031801 (2010).
19. Y.D. Chong, L. Ge, and A.D. Stone, "PT-symmetry breaking and laser-absorber modes in optical scattering systems," Phys. Rev. Lett. **106**, 093902 (2011).
20. H. Ramezani, T. Kottos, R. El-Ganainy, and D. N. Christodoulides, "Unidirectional nonlinear PT-symmetric optical structures," Phys. Rev. A **82**, 043803 (2010).
21. J. Schindler, Z. Lin, J. M. Lee, H. Ramezani, F. M. Ellis , and T. Kottos, "PT-symmetric electronics," J. Phys. A -Math and Theor. **45**, 444029 (2012).
22. H. Ramezani, J. Schindler, F.M. Ellis, U. Günther, and T. Kottos, "Bypassing the bandwidth theorem with PT symmetry," Phys. Rev. A **85**, 062122 (2012).
23. Z. Lin, J. Schindler, F.M. Ellis, and T. Kottos, "Experimental observation of the dual behavior of PT-symmetric scattering," Phys. Rev. A **85**, 050101(R) (2012).
24. Y-F Xiao, M. Li, Y-C Liu, Y. Li, X. Sun, and Q. Gong, "Asymmetric Fano resonance analysis in indirectly coupled microresonators," Phys. Rev. A **82**, 065804 (2010).
25. B-B Li, Y-F Xiao, C-L Zou, X-F Jiang, Y-C Liu, F-W Sun, Y Li, and Q Gong, "Experimental controlling of Fano resonance in indirectly coupled whispering-gallery microresonators", Applied Phys. Lett. **100**, 021108 (2012).
26. Q. Xu, S. Sandhu, M. L. Povinelli, J. Shakya, S. Fan, and M. Lipson, "Experimental realization of an on-chip all-optical analogue to electromagnetically induced transparency," Phys. Rev. Lett. **96**, 123901 (2006).
27. K. Totsuka, N. Kobayashi, and M. Tomita, "Slow light in coupled-resonator-induced transparency," Phys. Rev. Lett. **98**, 213904 (2007).
28. D. D. Smith, H. Chang, K. A. Fuller, A. T. Rosenberger, and R. W. Boyd,"Coupled-resonator-induced transparency," Phys. Rev. A **69**, 063804 (2004).
29. A. E. Miroshnichenko, B.A. Malomed, and Y.S. Kivshar, "Nonlinearly PT-symmetric systems: spontaneous symmetry breaking and transmission resonances," Phys. Rev. A **84**, 012123 (2011).
30. J. Ctyroky, I. Richter, and V. Sinor, "Dual resonance in a waveguide-coupled ring microresonator," Optic. Quantum Electron. **38**, 781-797 (2006).

1. Introduction

The realization of micron scale photonic elements and their integration into a single chip-scale device constitute an important fundamental and technological challenge. A bottleneck towards their realization is the creation of on-chip optical isolators. Standard approaches for isolation rely mainly on magneto-optical (Faraday) effects, where space-time symmetry is broken via external magnetic fields. This approach requires large-size non-reciprocal structures which are incompatible with on-chip integration. Alternative proposals include dynamical modulation of the index of refraction [1], the use of opto-acoustic effects [2], and optical non-linearities [3–8] etc. Most of these schemes, have serious drawbacks which make them unsuitable for small-scale implementation. In some cases, complicated designs that provide structural asymmetry are necessary, or the transmitted signal has different characteristics (e.g frequency) than the incident one. In others, direct reflection or absorption dramatically affects the functionality leading to an inadequate balance between transmitted optical intensities and figures of merit.

Recently, optical microresonator structures [9] with high-quality factors that trigger non-linear effects, have attracted increasing attention as basic elements for the realization of on-chip optical diodes [7, 8]. The basic geometries used consists of two waveguides coupled with two single mode non-linear cavities. These geometries typically allow for a narrow band transmission channel with a symmetric Lorentzian transmittance lineshape. In [7], Fan et al. used a structure that was passive and the diode action was imposed due to the asymmetric coupling of the cavities to the waveguides. The drawback of this protocol is that a high degree of asymmet-

#207316 - $15.00 USD Received 27 Feb 2014; revised 28 Mar 2014; accepted 30 Mar 2014; published 14 Apr 2014

ric transport (associated with to strong asymmetric coupling) is achieved at the expense of low intensity output signals due to transmission losses and strong direct reflections at the coupling points. On the other hand, the proposal of [8] by Peng et al. involved active cavities (one with gain and another with loss) where gain in the first resonator is supplied by optically pumping Erbium ions embedded in a silica matrix while the second resonator exhibits passive loss. As it was theoretically predicted in [10] by Bender et al., by using analogies with electronic circuit theory, such a set up excites the nonlinear resonances differently, depending on the incident direction, thus leading to strong asymmetric transport. We stress that the main advantage of the active scheme is that the losses in transmission are no longer an issue because they are compensated by the gain element.

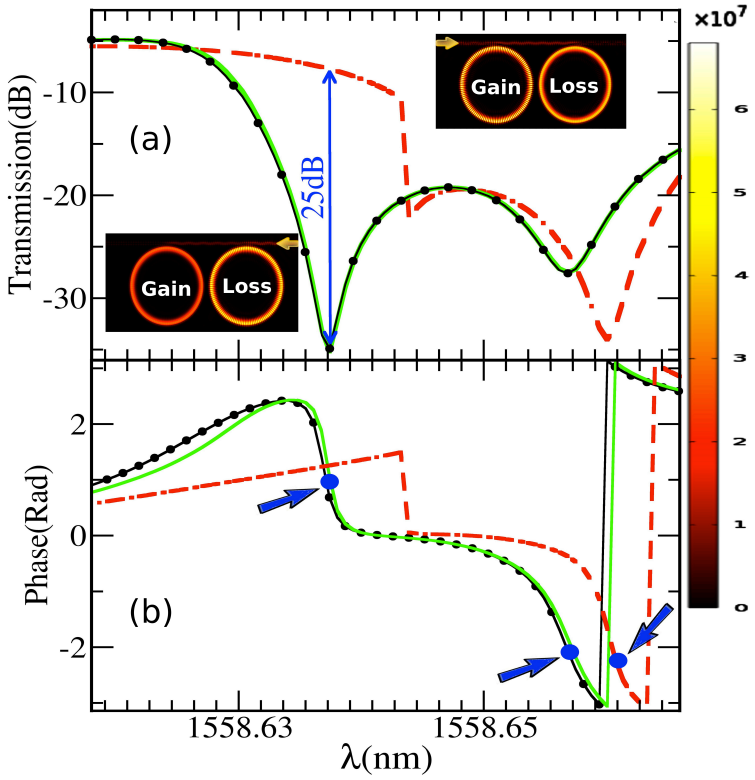

Fig. 1. (a) The transmittances $T(\lambda)$ of the linear system for incident waves from the gain (filled black circles) and from the loss (black line) side are compared with the corresponding $T(\lambda)$ in the case of microdisks with Kerr non-linearity. The resonance from the loss side (green line) experienced a small red-shift with respect to the linear structure. In contrast, the transmittance curve (both line-shape and resonance position) of an incident wave entering the structure from the gain side (red dotted-dashed line) is different. Insets: Schematic of the photonic circuit. The color coding indicates the intensity strength of the field inside the circuit. (b) The transmission phases (taken in the interval $[-\pi,\pi]$) are plotted as a function of wavelength λ. The colors and the line-type indicate the same scattering process as the one used in the upper panel. The blue arrows (and the blue dots) mark the wavelengths for which we have the Fano resonances.

In this paper we utilize *directional nonlinear Fano resonances*, emerging in a photonic circuit consisting of two non-linear $\mathscr{P}\mathscr{T}-$symmetric microcavities which are side-coupled to a

#207316 - $15.00 USD Received 27 Feb 2014; revised 28 Mar 2014; accepted 30 Mar 2014; published 14 Apr 2014

waveguide, in order to create asymmetric transport. Specifically we show that due to the interplay of non-linearity with the active elements the generated nonlinear Fano resonances [11] are triggered at different resonance frequencies depending on the direction of the incident light. At the same time the $\mathscr{P}\mathscr{T}$-symmetric configuration, used in our scheme, provides a strong output signal and guaranties the stability of the circuit against lasing action.

2. The theoretical set-up

A realization of the proposed diode is shown in the inset of Fig. 1(a). For demonstration purposes, we assume the core of the waveguide and of the two microdisks to be AlGaAs. The permittivity of both microdisks and of the waveguide is taken to be $\varepsilon' = 11.56$ while the Kerr coefficient for the microdisks is $\chi = 1e-19(m^2/V^2)$. The radius of the mircrodisks and their distance between each other are $5\mu m$ and $770nm$, respectively. The width of the waveguide and its coupling distance to the resonators are $460nm$ and $120nm$, respectively. We consider wavelengths around $\lambda \approx 1558.64nm$ at the optical communication window with one disk experiencing gain, while the other one having an equal amount of loss described by the imaginary part of the permitivity $\varepsilon'' = 0.00063$. The quality factors Q for the gain and loss microdisks at the above frequency were evaluated numerically using the Mode Analysis package of COMSOL and were found to be $Q_{\rm G} = 5.2\times 10^5$ for the gain disk and $Q_{\rm L} = 4.9\times 10^5$ for the lossy disk respectively. Note that the calculations reported below are two-dimensional. The "effective mode" surfaces $S_{\rm sur} = \int_{\rm surface,\mathscr{S}} \varepsilon(\mathbf{r})\,|\mathbf{E}(\mathbf{r})|^2\, d\mathscr{S}/\max[\varepsilon(\mathbf{r})\,|\mathbf{E}(\mathbf{r})|^2]$ were calculated using the method proposed in [12] and were found to be $S_{\rm sur} \approx 9\mu m^2$ for both microdisks.

The proposed structure is invariant under $\mathscr{P}\mathscr{T}-$ symmetry where the $\mathscr{P}$ is the parity reflection, with respect to the axis of symmetry of the two resonators, and $\mathscr{T}$ is the time reversal operator which turns loss to gain and vice versa. The concept of $\mathscr{P}\mathscr{T}-$symmetry first emerged within the context of mathematical physics. In this regard, it was recognized that a class of non-Hermitian Hamiltonians that commute with the $\mathscr{P}\mathscr{T}$ operator may have entirely real spectra [13]. As the degree of the non-Hermiticity, controlled by some balanced gain and loss mechanism, is increasing towards some critical value a spontaneous $\mathscr{P}\mathscr{T}$ -symmetry breaking can occur. Beyond this critical point the spectrum becomes partially or completely complex despite the fact these Hamiltonians and the $\mathscr{P}\mathscr{T}$ operator continuous to commute. The latter phase is known as *broken* $\mathscr{P}\mathscr{T}$-symmetric phase while the former is known as *exact* $\mathscr{P}\mathscr{T}$-symmetric phase. The "phase transition" point between the two regimes is termed spontaneous $\mathscr{P}\mathscr{T}$-symmetry point and has all the characteristics of an exceptional point [14].

Lately, these notions have successfully migrated and observed in other areas like photonic [15–20] and electronic circuitry [10, 21–23]. One of the interesting findings is the fact that a $\mathscr{P}\mathscr{T}$-symmetric cavity can have singular frequency points for which the transmission/reflection coefficients are diverging (laser action) or become zero for appropriate phase and amplitude arrangements of the incident waves (Coherent Perfect Absorber) [18, 19]. The experimental confirmation of this idea was recently demonstrated in the framework of $\mathscr{P}\mathscr{T}$-electronics [21]. One needs to be aware that these singular points for which the cavity is unstable (e.g. lasing) are deep inside the broken phase. For other parameter values inside the broken phase (but not in the immediate neighborhood of these points), a $\mathscr{P}\mathscr{T}$ -system is stable and operates as a simple amplifier (but not a laser) [18, 19, 21].

In all our simulations below we have considered parameters (gain and loss parameter and coupling) such that the system of Fig. 1(a) is in the broken phase but away from any lasing point. The direct coupling between the two microdisks is controlled via their distance and in our case is very weak. We have checked this by numerical simulations where in the absence of the bus waveguide an excitation in one of the disks will remain essentially there and will not couple to the other resonator. A "weak" indirect coupling between the microdisks is then

#207316 - $15.00 USD Received 27 Feb 2014; revised 28 Mar 2014; accepted 30 Mar 2014; published 14 Apr 2014

established via their proximity to the bus waveguide. The importance of indirect coupling and its implications to the formation of Fano resonances has been theoretically understood in [24] by Xiao et al. and experimentally confirmed in [25] by Li et al. This arrangement ensures that the system is in the broken phase. We will show that the interplay of the stability (e.g. non-lasing) and amplification properties of $\mathscr{P}\mathscr{T}$-symmetric systems in the broken phase together with the presence of non-linearity can result in unidirectional amplified transport.

2.1. Numerical simulations

In Fig.1(a) we show, for the photonic circuit shown in the inset, some transport simulations using COMSOL modeling. The input power used is $P = 1.2mW$. We find that the left-to-right transmittance $T_L(\lambda)$ differs from the right-to-left transmittance $T_R(\lambda)$, i.e. $T_L \neq T_R$ and thus the proposed set-up can act as an optical isolator. The asymmetry is most pronounced near the Fano resonances $\lambda_{\chi=0}^{\mathscr{P}\mathscr{T}}$ of the linear $\mathscr{P}\mathscr{T}$-symmetric structure, and constitutes our main result. We stress that non-reciprocal transport is forbidden by the Lorentz reciprocity theorem in the case of linear, time-reversal symmetric systems. Also, it cannot be achieved by a conservative nonlinear medium by itself nor by linear $\mathscr{P}\mathscr{T}$-symmetric structures (black circles and black line in Fig. 1(a)) [23].

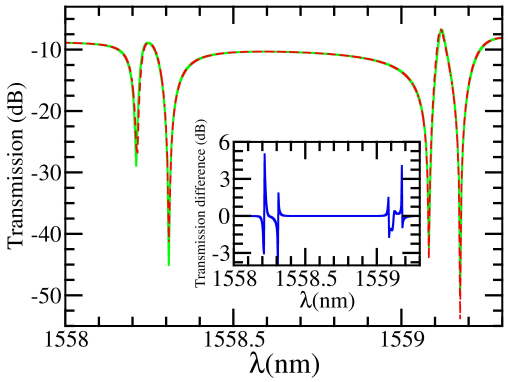

Fig. 2. The transmittances $T(\lambda)$ for a left (red curve) and right (green curve) incident light for the non-linear system shown in Fig. 1(a). The frequency window contains two Fano resonances. Here the two microdisks are placed in distance $100nm$ so that the system is in the exact phase. In the inset we report the difference between left and right transmittances. The maximum asymmetry that has been found is as high as 5.5dBs. This has to be contrasted with the case of Fig. 1(a) where the system is in the broken phase and the maximum asymmetry reached values as high as 25dBs.

The creation of Fano resonances is not a surprise. Similar configurations where the microdisks were passive have been already investigated in the past (see for example [11,25,26,28]) and Fano resonances were found. Their origin was traced to coherent interferences between two scattering processes: the first involves scattering within a continuum of states (associated with the channel modes supported by the bus waveguide) while the second is a resonant process and involves the excitation of a discrete resonance mode of the micro-resonators that has an associated frequency within the continuum of states supported by the waveguide. In the neighborhood of the resonance frequency the resonant scattering amplitude (in contrast to the amplitude associated with the continuum process) undergoes sharp variations both in magnitude and in phase. Specifically, as can be seen from Fig. 1(b), within a frequency interval proportional to the resonance line-width, the phase of the resonant scattering amplitude changes rapidly by π leading

#207316 - $15.00 USD Received 27 Feb 2014; revised 28 Mar 2014; accepted 30 Mar 2014; published 14 Apr 2014

to destructive interference effects and consequently to an asymmetric transmittance profile. At frequencies further away from the resonance frequency the direct scattering via the continuum states is the dominant scattering mechanism and controls the shape of the transmittance. When the second microresonator is attached to the bus-waveguide, the asymmetry in the transmittance profile can further enhanced and a transparent frequency window can emerge. The origin of this Electromagnetically Induced Transparency (EIT) is related to the interaction between nearby (e.g. their frequency difference is of the order of their line-width) Fano resonances and it is controlled by an additional phase accumulation associated with the distance between the two resonators.

Here we would also like to mention that asymmetric transport can be achieved also in the exact phase where the eigenfrequencies of the corresponding closed (isolated) system are real (for the definition of the exact phase see also introduction in section 2 and related comment in [14]). However in this case the degree of asymmetry between left and right incident light is very small. An example case of such weak asymmetric transport is reported in Fig. 2. Here the maximum observed asymmetry (see inset) is as high as 5.5dBs which has to be contrasted with the 25dBs exhibited by the system when it is in the broken phase (see Fig. 1(a)). The parameters used in these numerical simulations are the same as in Fig. 1(a) apart from the distance between the microdisks which now is taken to be $100nm$ so that the system is in the exact phase.

We want to analyze the origin of the asymmetry between left and right transmittances, near the Fano resonances $\lambda_{\chi=0}^{\mathscr{P}\mathscr{T}}$ of the linear photonic circuit of Fig. 1(a). To understand better its origin, we first discuss the transport characteristics of a single gain (lossy) non-linear microdisk side-coupled to a waveguide. In the case that the incident light traveling the waveguide couples with a gain resonator it will be amplified substantially because of the interaction with the gain medium, and the high Q factor of the disk. Consequently, the signal has sufficiently high power to trigger the non-linearity and red-shift the disk's resonance λ_{χ}^{G}, thus allowing it to pass with small (or even not at all) attenuation at the resonance wavelength $\lambda_{\chi=0}^{G}$ of the gain cavity (dashed red line in Fig 3(a)). On the other hand, when light couples to a lossy microdisk, the optical energy stored in this disk is not high enough to appreciably red-shift (via non-linearity) the resonance because of the power reduction due to the losses. As a result the transmittance has a resonance dip at $\lambda \approx \lambda_{\chi=0}^{L}$. Obviously in both cases discuss here, we have $T_L(\lambda) = T_R(\lambda)$.

Next we investigate the transmission spectra of the combine system of the two microdisks side coupled to the bus waveguide. In Fig. 3(b) we compare the transmission for different configurations of gain and loss in the absence of nonlinearity and for the same frequency window. First we note that in the absence of any gain and loss (black line) the system of the two microdisks have a resonance around $\lambda = 1558.65nm$. Introducing loss to one of them (maroon line with open circles) leads to a decrease of the quality factor and thus further broadening of the resonance. In case that additional loss is introduced to the second resonator as well (green line) the quality factor drops further down and the resonance width becomes broader. Obviously, in both of these cases the transmittance decreases with respect to the passive case and we always have that $T_L(\lambda) = T_R(\lambda)$.

When the lossy micro-disk (right) is balanced with a gain microdisk (right) and both are side-coupled to the bus waveguide, two Fano resonances emerge. Moreover $T(\lambda)$ shows a peak in the middle of the resonant dip (see red dashed line in Fig. 3(b)). This phenomenon is an optical analogue [26, 27] of electromagnetically induced transparency (EIT) and it is known as *coupled-resonator-induced transparency* [28]. It is associated with the interaction between two Fano resonances with spectral widths which are comparable to or larger than the frequency separation between them. Still we observe that $T_L(\lambda) = T_R(\lambda)$.

In Fig. 3(c) we report the effect of nonlinearity on the transmittance profiles for the same low incident power as the one used in Fig. 1(a). First we notice that for a passive structure the res-

#207316 - $15.00 USD Received 27 Feb 2014; revised 28 Mar 2014; accepted 30 Mar 2014; published 14 Apr 2014

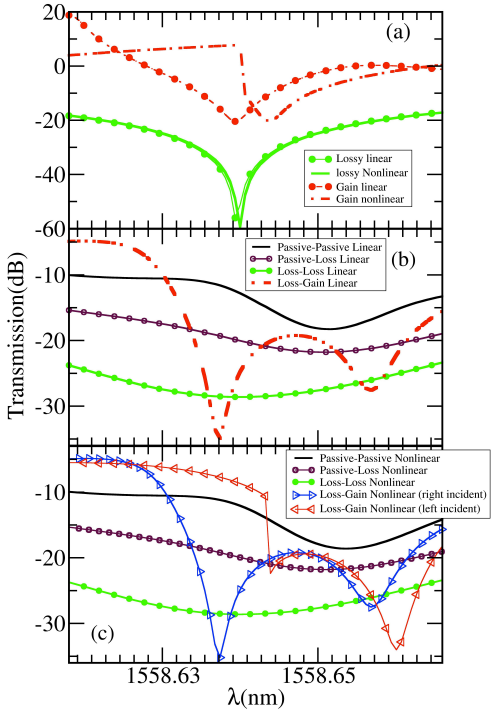

Fig. 3. (a) Transmittances $T(\lambda)$ for a single gain or loss microdisk coupled to a waveguide. The filled green circles (green line) correspond to a lossy disk in the absence (presence) of Kerr nonlinearity. The filled red circles (dotted-dashed line) correspond to a gain disk in the absence (presence) of Kerr nonlinearity. A red-shift of the resonance position and a strong modification of $T(\lambda)$ is observed. (b) The transmission spectra of two coupled linear microdisks with various gain and loss configurations (see legends in the figure). (c) The same as in (b) but now the two microdisks have a Kerr non-linearity. In the $\mathscr{PT}$-symmetric configuration we report the transmission spectra for both left (gain side) and right (loss side) incident beams.

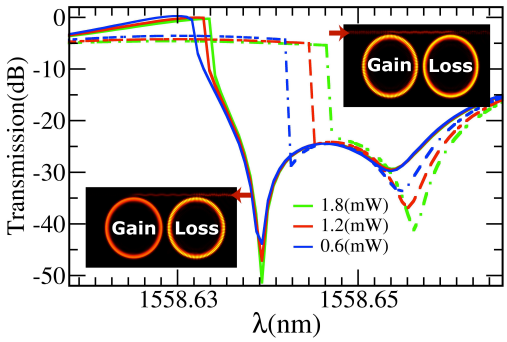

Fig. 4. Transmittance for different input powers. The asymmetric transport is maintained for a broad range of input power levels. Dashed lines correspond to $T_L(\lambda)$ (gain side) while solid lines to $T_R(\lambda)$ (lossy side). The transport asymmetry is as high as 46.5 dB without compromising the outgoing optical intensity which is as high as -5 dBs.

#207316 - $15.00 USD Received 27 Feb 2014; revised 28 Mar 2014; accepted 30 Mar 2014; published 14 Apr 2014

onance frequency experiences a weak red-shift in comparison to its linear analogue (compare the black lines in Figs. 3(b) and 3(c)). This red-shift is even weaker in the presence of losses (compare maroon and green lines in Figs. 3(b) and 3(c)). Again in this case we find symmetric transport. We therefore conclude that non-linearity (in a passive structure) by itself cannot generate asymmetric transport. In order for this to happen one needs to break the parity symmetry in the system [5–8, 10].

When we use a $\mathscr{P}\mathscr{T}$-symmetric configuration together with non-linearities (see red and blue curves in Fig. 3(c)), we observe a dramatic difference with respect to the linear case (red line in Fig. 3(b)). Namely now $T(\lambda)$ near the Fano resonances is not only asymmetric but its shape also depends strongly on the direction of the incident light. Below we focus on wavelengths on the left of the transparent window where, for our theoretical design, the asymmetry is stronger. In this case the light entering the waveguide from the left is first coupled to the gain resonator which amplify the light intensity; thus inducing optical nonlinearity of the material. As a result, the resonance wavelength $\lambda_{\chi}^{\mathscr{P}\mathscr{T}}$ of the non-linear $\mathscr{P}\mathscr{T}$-structure is strongly red-shifted with respect to the resonance wavelength $\lambda_{\chi=0}^{\mathscr{P}\mathscr{T}}$ of the linear $\mathscr{P}\mathscr{T}$-circuit. Thus at incident wavelength $\lambda=\lambda_{\chi=0}^{\mathscr{P}\mathscr{T}}$ the photonic circuit of Fig. 1(a) is almost transparent. Moreover, the outgoing signal is strong due to the amplification at the gain disk and despite the fact that some attenuation will take place at the lossy resonator. For backward propagation, light will first couple to the lossy resonator where it will experience attenuation. When the light reaches the gain microdisk, the accumulated energy there is not enough to appreciably red-shift the resonance. Thus light is transmitted to the left port through the resonance and experience a transmission dip at $\lambda_{\chi=0}^{\mathscr{P}\mathscr{T}}$. Therefore a non- reciprocal light transport at $\lambda_{\chi=0}^{\mathscr{P}\mathscr{T}}$ is observed. The asymmetric transport is further amplified due to the different Fano lineshape for a left and right incident waves.

In Fig. 4 we analyze the dependence of $T(\lambda)$ on the level of the input power. We find that the proposed circuit is stable to variations of the input power; a feature that is desirable from the engineering perspective. For these simulations we assume an imaginary permittivity $\varepsilon''=0.00073$, i.e. slightly larger than the one used in Fig. 1(a), which results in enhanced transport asymmetry (46.5 dBs). At the same time the outgoing signal $T_L(\lambda=\lambda_{\chi=0}^{\mathscr{P}\mathscr{T}})$ is amplified (≈ -5 dBs) with respect to the one found in Fig. 1(a) (≈ -8 dBs). This has to be contrasted with passive protocols where an increase figure of merit for isolation might lead to weaker outgoing signal [5, 7].

2.2. *A simple theoretical model: the non-linear $\mathscr{P}\mathscr{T}$-symmetric Fano model*

The asymmetric transport generated by the interplay of the nonlinear Fano resonances with $\mathscr{P}\mathscr{T}$-symmetric elements calls for a simple theoretical understanding. The following heuristic model, similar in spirit to the so-called Fano-Anderson model that is used to describe the creation of (non-linear) Fano resonances [11, 29], provides some quantitative understanding of the COMSOL simulations shown in Figs. 1(a),4. Our model is described by the following equations:

$$\begin{aligned} i\dot{\phi}_n &= -\{C(\phi_{n-1}+\phi_{n+1})+V_G\phi_G\delta_{n,0}+V_L\phi_L\delta_{n,N}\} \\ i\dot{\phi}_{G/L} &= -\{(E\mp i\gamma)\phi_{G/L}+\chi|\phi_{G/L}|^2\phi_{G/L}+V_{G/L}\phi_{0/N}\} \end{aligned} \tag{1}$$

Equations (1) describe the interaction of two subsystems. The first one is a linear chain of couple sites with coupling constant C and on-site complex field amplitudes ϕ_n. This system supports propagating plane waves with dispersion $\omega(k)=2Ccosq$ and models the bus waveguide of the configuration shown in the inset of Fig. 1(a). The second subsystem consists of two defect states ϕ_G (gain) and ϕ_L (loss) with on-site energy $E\mp i\gamma$ respectively and models the resonance modes associated with the two micro-resonators (one with gain and the other with loss) of Fig. 1(a).

#207316 - $15.00 USD Received 27 Feb 2014; revised 28 Mar 2014; accepted 30 Mar 2014; published 14 Apr 2014

The two subsystems interact with one another at the sites $n = 0, N$ via the coupling coefficients $V_{G/L}$. This coupling element models the evanescent coupling between the resonance modes of each microdisk and the bus waveguide in the set-up shown in the inset of Fig. 1(a). We note that our model Eq. (1) assumes zero direct coupling between the gain and loss sites in complete analogy with the proposed photonic circuit of Fig. 1(a). Nevertheless, an indirect coupling between the two defects is maintained via the linear chain, due to backscattering processes at the intersection points where the defects are coupled to the chain. This indirect coupling is also present in the case of our set-up shown in Fig. 1(a) as discussed previously. In this case, a backscattering mechanism caused by the coupling section between each cavity and the bus waveguide [30] excites both clockwise (CW) and counterclockwise (CCW) modes and enforces energy exchange between the two microdisks [24, 25].

We assume elastic scattering processes for which the stationary solutions take the form $\phi_n = A_n e^{i\omega t}$; $\phi_G = A_g e^{i\omega t}$; $\phi_L = A_L e^{i\omega t}$. Substitution in Eqs. (1) leads to

$$\begin{aligned} \omega A_n &= C(A_{n-1} + A_{n+1}) + V_G A_G \delta_{n,0} + V_L A_L \delta_{n,N} \\ \omega A_{G/L} &= E A_{G/L} \mp i\gamma A_{G/L} + \chi |A_{G/L}|^2 A_{G/L} + V_{G/L} A_{0/N} \end{aligned} \tag{2}$$

We consider a left incident wave. In this case we have

$$A_n = \begin{cases} I e^{iqn} + r e^{-iqn} & n \leq 0 \\ \alpha e^{iqn} + \beta e^{-iqn} & 0 \leq n \leq N \\ t e^{iqn} & N \leq n \end{cases} \tag{3}$$

where I, r, t represent the incident, reflected and transmitted wave amplitudes far from the defect sites. Substituting the above scattering conditions in Eqs. (2) and using the continuity conditions at the defect sites $n = 0, N$, we get after some straightforward algebra

$$r_L = i\frac{V_G A_G + V_L A_L e^{iqN}}{2C \sin q}; \quad t_L = (I + i\frac{V_G A_G + V_L A_L e^{-iqN}}{2C \sin q}) \tag{4}$$

The unknown amplitudes A_G, A_L can be found in terms of the input amplitute I by utilizing Eqs. (2). Specifically we get the following set of nonlinear equations

$$(E - \omega - i\gamma)A_G + \chi |A_G|^2 A_G + V_G(I + r_L) = 0; \quad (E - \omega + i\gamma)A_L + \chi |A_L|^2 A_L + V_L e^{iqN} t_L = 0 \tag{5}$$

which can be solved numerically, after substituting r_L and t_L from Eqs. (4).

The transmittance and reflectance for a left incident wave is defined as $T_L = |t_L/I|^2$ and $R_L = |r_L/I|^2$ respectively. In a similar manner one can also define the transmittance $T_R = |t_R/I|^2$ and reflectance $R_R = |r_R/I|^2$ for a right incident wave. The associated t_R, r_R are given by the same expressions as Eqs. (4, 5) with the substitution of $\gamma \to -\gamma; V_G \to V_L$ and $V_L \to V_G$.

An analysis of the structure of Eq. (4) can explain the origin of Fano resonances. Specifically, we note that the transmission amplitude in Eq. (4) consists of two terms: the first one is associated with a propagating wave that directly passes through the chain without coupling to any of the defect states. The second term describes an indirect path for which the wave will first visit the two defects, thus exciting the Fano states, return back, and continue with the propagation. These two paths are the ingredients of the Fano resonances observed in Figs. 1(a) and 4. Finally we note the importance of the propagation distance N between the two defect modes G/L which appear in Eq. (4) in the form of the additional phase $\exp(-iqN)$. This additional phase is responsible for the incomplete constructive interferences associated with the EIT window. The resulting EIT resonance is formed via constructive interferences associated with photon trajectories inovolving multiple scattering processes between the two defect modes.

#207316 - $15.00 USD Received 27 Feb 2014; revised 28 Mar 2014; accepted 30 Mar 2014; published 14 Apr 2014

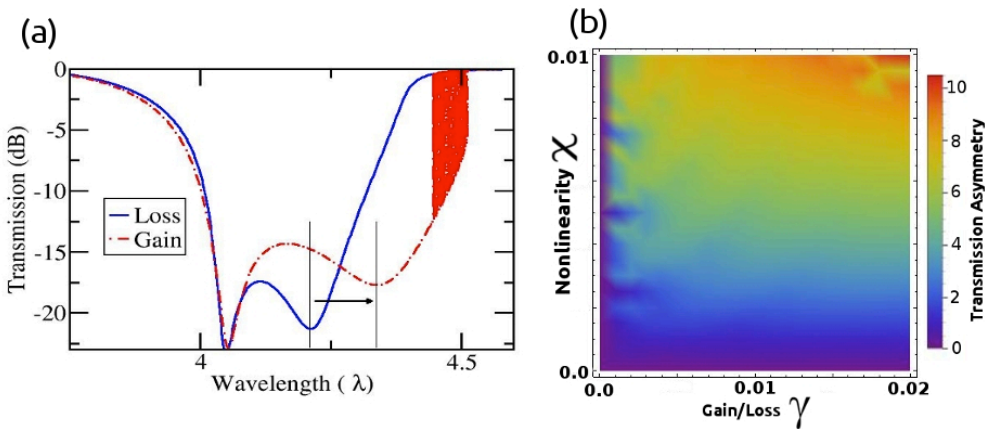

Fig. 5. (a) Left (gain) T_L and right (loss) T_R transmittances for the theoretical model of Eq. (1). Notice the red-shift associated with T_L (pointed with a black arrow), in the neighborhood of the second Fano resonance. In this domain the asymmetry is most pronounced $T_L \neq T_R$. The parameters used in this simulation are $V_G = V_L = 0.5$, $N = 1$, $\chi = 0.0125$ and $\gamma = 0.02$. The red-shadowed area on the right of the graph around $\lambda \approx 4.5$, corresponds to a bi-stability behavior which however is away from the Fano resonance regime and thus does not affect asymmetric transport. (b) A density plot of the transmission asymmetry $10|\log_{10}(T_L) - \log_{10}(T_R)|$ versus the gain and loss parameter γ and the non-linearity χ. The maximum asymmetry is observed for large values of χ and γ (upper right corner of the $\chi - \gamma$ parameter space).

In Fig. 5(a) we report a representative set of transmission curves for a left/right incident wave for the model of Eq. (1). The model captures the qualitative features and origin of the asymmetric transport observed in the case of the photonic circuit of Fig. 1(a). Specifically, we find that both the shape and the position of the Fano resonances depend on the direction of the incident wave. Moreover for a left (gain-side) incoming wave, a red-shift in the transmittance resonances is found (see the second Fano resonance in Fig. 5(a)). We have found that in the frequency domain around this resonance the asymmetry in the transmittances gets the maximum value.

We also report, in Fig. 5(b), a density plot of the transmission asymmetry between T_L and T_R (measured in dBs) versus the non-linearity strength χ and the gain and loss parameter γ. In the simulations presented here we made sure, that the values of the non-linearity and the gain and loss parameter are always considerably below the critical value that triggers multi-stabilities within the frequency domain where the Fano resonances appear (highlighted area on the right of Fig. 5(a)). The results of our simple mathematical model of Eq. (1) reconfirm the predictions of the numerical simulations of the photonic circuit. Namely we find that increase of the non-linearity and the gain and loss parameter can result in higher values of asymmetry (upper right corner of Fig. 5(b)).

3. Conclusions

In conclusion, we utilized $\mathscr{P}\mathscr{T}$-symmetric Fano resonances with a line-shape and a resonance position that depends on the direction of the incident wave in order to achieve asymmetric transport. The proposed photonic circuit that allows for such resonances consists of two $\mathscr{P}\mathscr{T}$-symmetric microdisks side-coupled to a waveguide. Although there are proposals involving passive structures that can achieve high asymmetric transport (see for example [7]), the merit

#207316 - $15.00 USD Received 27 Feb 2014; revised 28 Mar 2014; accepted 30 Mar 2014; published 14 Apr 2014

of our configuration is that it can simultaneously guarantee high degree of asymmetric transport (due to the interplay of non-linearity and $\mathscr{P}\mathscr{T}$-symmetry) and strong output signal (due to the directional amplification of light provided by the interplay of the properties of $\mathscr{P}\mathscr{T}$-symmetric systems in the broken phase and non-linearity).

Our proposal utilizes materials already used in optical integrated circuitry processing and does not require magnetic fields. The efficiency of the asymmetric transport for a broad input power range and low values of input power within which our proposed scheme performs may be sufficient for on-chip photonic applications. A problem with the simple design of Fig. 1(a) is that the asymmetric transport only occurs in the vicinity of the Fano resonances (narrow band). This problem can be addressed by using more sophisticated photonic structures, for instance, those involving more than one $\mathscr{P}\mathscr{T}$-symmetric dimer-like resonators side coupled to the waveguide bus.

Acknowledgments

HR, DNC and TK acknowledge partial support from an AFOSR MURI grant FA9550-14-1-0037 and an NSF ECCS-1128571 grant. TK acknowledges partial support from DFG Forschergruppe 760. NB acknowledges support from a REU NSF ECCS-1128571 grant. FN research was supported from a Wesleyan project grant (Dean's office).

#207316 - $15.00 USD Received 27 Feb 2014; revised 28 Mar 2014; accepted 30 Mar 2014; published 14 Apr 2014